RETURN TO 1998 ROD AR INDEX

Superfund Records Center
SITE: NEW BEDFORD
BREAK: 17.07
OTHER: 274578

Environ. Sci. Technol. 1991, 25, 760–770

Application of a Food Chain Model to Polychlorinated Biphenyl Contamination of the Lobster and Winter Flounder Food Chains in New Bedford Harbor

John P. Connolly

HydroQual, Inc., 1 Lethbridge Plaza, Mahwah, New Jersey 07430 and Environmental Engineering and Science Program, Manhattan College, Riverdale, New York 10471

■ As part of a Remedial Investigation/Feasibility Study for the New Bedford Harbor Superfund site a model of polychlorinated biphenyls (PCBs) in the lobster and winter flounder food chains was developed. This model successfully reproduces tri-, tetra-, penta-, and hexachlorobiphenyl concentrations observed at all levels of the food chain and across the 2 order of magnitude concentration gradient in the system. The model indicates that PCB concentrations in the flounder and, to a lesser extent, in the lobster are derived from the sediment. Dietary uptake exceeds uptake across the gill for all four homologues and becomes the dominant route at the higher chlorinated homologues. The assimilation efficiency of ingested PCB apparently declines from relatively high values for trichlorobiphenyl to relatively low values for hexachlorobiphenyl. Differences in observed lobster and flounder PCB concentrations appear to be due to differences in the importance of the benthic component of the food chains of these animals and differences in whole body lipid content.

Introduction

From the 1940s to the late 1970s New Bedford Harbor, a tidal estuary located at the head of Buzzards Bay in southeastern Massachusetts, received PCB-containing industrial wastewaters from two electronic component manufacturing plants. These discharges resulted in PCB concentrations in sediments that ranged as high as 100 000 ppm and concentrations in biota that exceeded the Food and Drug Administration (FDA) action limit of 2 μg/g (previously 5 μg/g). As a result of this PCB contamination, finfish and shellfish fisheries in the harbor and in bordering areas of Buzzards Bay have been closed since 1979. Of particular concern in this regard are the lobster and winter flounder, whose fisheries are economically important to the area. The region has been designated as a "SuperFund Site" and a Remedial Investigation/Feasibility Study (RI/FS) has recently been completed. As part of this study, a model of PCB homologues 3–6 in the lobster and winter flounder food chains was developed and applied to the harbor and Buzzards Bay. This model is an extension of a modeling framework previously applied to food chains in Lake Michigan (*1*) and in the James River estuary (*2*). It is the first attempt to model multiple chemicals in a system exhibiting a significant spatial contamination gradient. As such it is a rigorous test of the model formulation.

The model has been successfully calibrated to data collected as part of the RI/FS. Calibration was achieved with a single set of bioenergetic parameters and assimilation efficiency and excretion rates were defined by literature-based relationships to the octanol/water partition coefficient (K_{ow}). It is the purpose of this paper to present the modeling framework and the calibration and to discuss the importance of various processes to the accumulation of PCBs, and to hydrophobic organic chemicals in general.

PCB Contamination in New Bedford Harbor

PCB measurements prior to 1979 of water, sediment, and biota in New Bedford Harbor revealed a significant concentration gradient. Highest concentrations were observed in the upper estuary, declining downriver and through an outer harbor area into Buzzards Bay (study area is shown in Figure 1). Consistent with this gradient, the fishery closure established in 1979 by the Massachusetts Department of Public Health is divided into three areas. The area north of the hurricane barrier (i.e., the inner harbor, area 1) is closed to the taking of all finfish, shellfish, and lobsters. The outer harbor (area 2), extending from the hurricane barrier to a line from Wilber Point to Ricketsons Point, is closed to the taking of lobster and bottom-feeding finfish including eel, scup, flounder, and tautog. Between the outer harbor and a line from the southern tip of West Island to Round Hill Point (area 3) only the lobster fishery is closed. Food chains were considered for each of the closure areas. In addition, a fourth area representative of the Buzzards Bay region south of area 3 was modeled. Area 1 is restricted to the region between the hurricane barrier and the Route 6 bridge, the area assumed to be the habitat of the species of interest.

As part of the RI/FS, Battelle Ocean Sciences (*3*) conducted cruises in New Bedford Harbor and Buzzards Bay in September–October 1984, November–December 1984, and June–July 1985 to collect water column, sediment, and biota samples. These samples were analyzed for PCB congener concentrations and the results were reported on a homologue basis. For the purposes of the food chain model concentrations were averaged for each of the four areas. Because cruise to cruise variability was not great (*3*), concentrations were also averaged across cruises to establish a data set for calibration of the food chain model.

Water Column and Sediment Concentrations. Spatial profiles of the average and range of dissolved concentrations of PCB homologues 3–6 and total PCB are presented in Figure 2. A dramatic decline in PCB concentration is evident proceeding from the lower inner harbor (area 1) to Buzzards Bay (area 3). Over this region concentrations decline by a factor of ca. 30, from a total dissolved PCB concentration of ~70 to ~2 ng/L. Moving out into Buzzards Bay from area 3 to area 4, concentrations remain approximately constant. Surface sediment concentrations decline in similar fashion (Figure 3), although the rate of decline is less than for water column dissolved concentrations. From area 1 to area 3 concentrations decline from ~360 to ~25 μg/g of C, a factor of 14. Unlike the water column, sediment concentrations in area 4 are lower than in area 3. The average concentration of 10 μg/g of C is about the same factor below that observed in area 1 as found for dissolved PCB. Although limited measurements of water column particulate organic carbon are available to compute carbon-normalized water column particulate PCB, the computed averages indicate concentrations significantly less those observed in the surface

 0013-936X/91/0925-0760$02.50/0 © 1991 American Chemical Society

SDMS DocID 274578

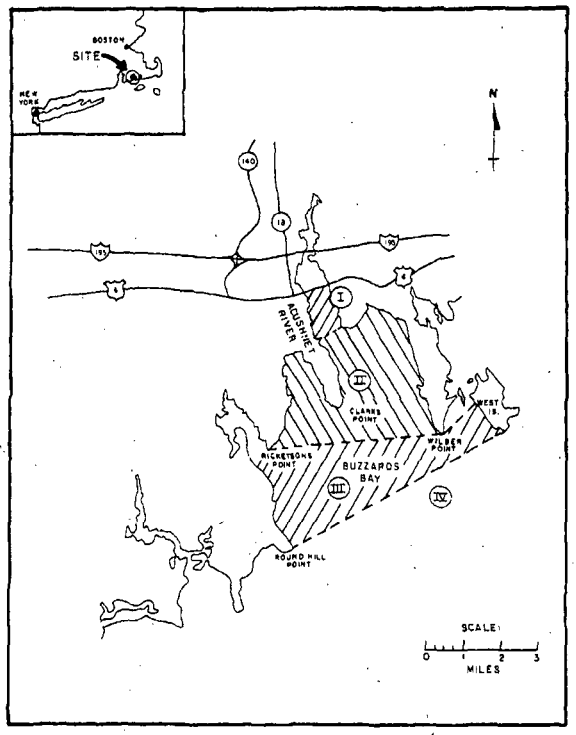

Figure 1. Study area. Roman numerals and hatching indicate the areas over which concentrations were averaged for the model.

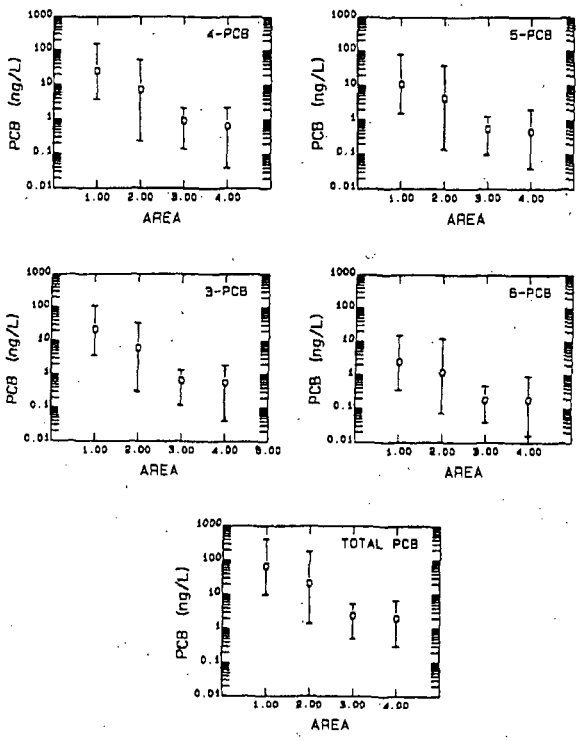

Figure 2. Average and range of dissolved PCB homologue concentrations in each of the four areas of New Bedford Harbor.

sediment. Values for the four areas, proceeding from area 1, are about 125, 45, 8, and 2 $\mu g/g$ of C, as compared to surface sediment values of 360, 160, 25, and 10 $\mu g/g$ of C. These differences between the water column and the

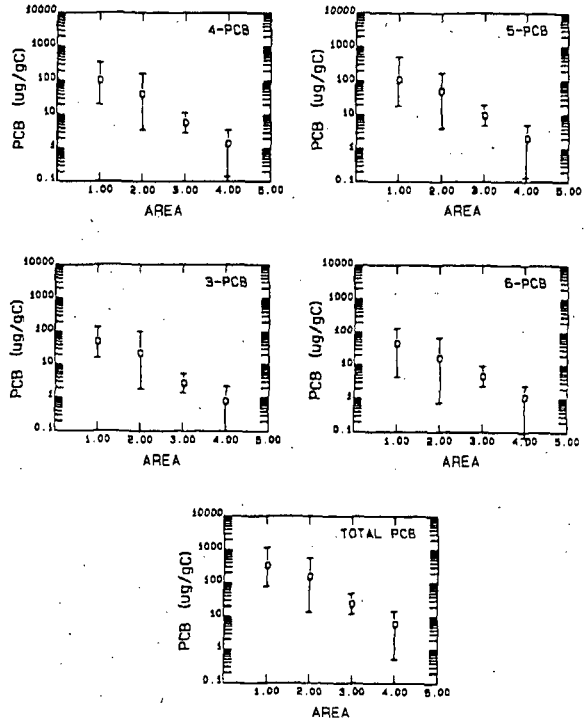

Figure 3. Average and range of surface sediment PCB homologue concentrations in each of the four areas of New Bedford Harbor.

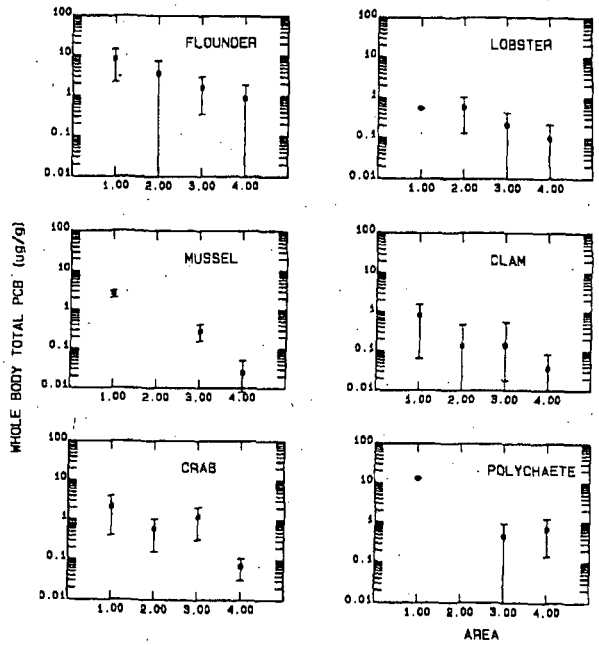

Figure 4. Average and range of biota whole body total PCB concentrations in each of the four areas of New Bedford Harbor.

sediment suggest that the system is depurating PCBs in response to cessation of active loading.

Concentrations in Biota. The spatial patterns of PCB concentration in polychaetes, hard clams, mussels, spider crabs, winter flounder, and lobsters are consistent with those observed for water and sediment. Figure 4 shows the average and range of whole body total PCB concentrations in each area of New Bedford Harbor for all the

species. Flounder and polychaetes exhibit the highest whole body concentrations, ~10 μg/g wet weight in area 1, probably reflecting their greater exposure to sediment PCBs. The lowest concentrations are found in the clam. Concentrations decline by factors of ~10–20 from area 1 to area 4. The pattern of decline differs somewhat from species to species. Both clams and crabs exhibit similar concentations in areas 2 and 3, whereas the concentrations in area 3 flounder and lobster are about 2 and 3 less than the values observed in area 2. Similarly, polychaete concentrations are about the same in areas 3 and 4 in contrast to the significantly lower values found in area 4 for all of the other species. These differences in the spatial pattern of PCB contamination probably reflect differences in PCB exposure. In particular, sedentary species collected in locations where the PCB exposure concentrations were much different from the area average concentration may not reflect the area to area patterns as well as mobile species whose exposure is integrated over a larger region.

Measurements of PCBs in flounder and lobster muscle tissue and in lobster hepatopancreas indicate a proportionality to whole body concentration that is independent of homologue. Average ratios are 1.35 for lobster muscle to whole body, 0.18 for flounder muscle to whole body, and 92 for lobster hepatopancreas to whole body (*3*). Thus, the 10 μg/g wet weight concentration in area 1 flounder is equivalent to ~2 μg/g of muscle, indicating that these flounder are at PCB levels about equal to the FDA action limit. For lobster, both the muscle and hepatopancreas are edible and conversion of whole body to edible tissue requires knowledge of the weight fractions of each. Limited data from the U.S. EPA Narragansett Laboratory (Richard Pruell, personal communication) indicate that muscle and hepatopancreas constitute about 91 and 9% of edible tissue, respectively. From these data, the lobster edible to whole body PCB concentration ratio is ~9.2. Thus, the maximum lobster concentrations of ~1 μg/g live weight (Figure 4) are equivalent to edible concentrations of ~9 μg/g, considerably above the FDA action limit.

Modeling of PCB Accumulation

Mass Balance Equation. The accumulation of toxic chemicals by aquatic animals may be described by the following equation (*1*):

$$\frac{dv_i}{dt} = K_{ui}c + \sum_{j=1}^{n} \alpha_{ij}C_{ij}v_j - (K_i + G_i)v_i \qquad (1)$$

where v_i is the concentration of chemical in species i in the food chain [μg/g(w), where g(w) is grams of wet weight]; K_{ui} is the rate constant for chemical uptake across the gill of species i [L/g(w)·day]; K_i is the rate constant for excretion of chemical by species i(1/day); α_{ij} is the efficiency at which ingested chemical from prey j is assimilated by species i; C_{ij} is the ingestion or consumption rate of species i on species j [g(w)prey (g(w)pred)$^{-1}$ day^{-1}]; G_i is the growth rate of species i [g(w) (g(w))$^{-}$ day^{-1}]; c is the dissolved chemical concentration (μg/L); and n is the number of species (including different year classes of a single species) preyed on by species i.

The first term of eq 1 represents the direct uptake of chemical by the animal from water. The second term represents the flux of chemical into the animal through feeding. The third term is the loss of chemical due to desorption and excretion plus the change in concentration due to growth. Equation 1 is applied to each of the animals that comprise the food chain. For the upper levels of the food chain, changes in chemical concentration with age are sometimes significant and each year class of the species at these levels is modeled separately.

The calculation is driven by externally specified concentrations of water column dissolved chemical and sediment dissolved and particulate chemical. The sediment particulate organic carbon is the base of the benthic food chain. The base of the pelagic food chain is water column phytoplankton. Chemical concentration in phytoplankton is calculated from the water column dissolved concentration by the use of a partition coefficient.

Food Chain Structure. Determination of the appropriate species to include in the model is based on a review of published stomach content data for lobster and flounder. From these data species are chosen to represent the next lower level of their food chains. Representative species are then chosen for each lower trophic level in succession to the phytoplankton–detritus level. At any level a single species is sometimes sufficient because the members of that level generally have similar bioenergetic characteristics and chemical concentrations. Additional prey animals are incorporated as necessary to account for differing prey chemical concentrations or multiple vectors of chemical transfer to the predator (i.e., sediment vs water column).

The lobster is the top predator in a three-level food chain. Stomach content analyses have indicated that small crustaceans, molluscs, polychaetes, and echinoderms are the main constituents of the diet of *Homarus americanus*. Studies of lobsters in Bonavista Bay, NF (*4*) and in Long Island Sound (*5*) indicate that crabs and molluscs (particularly mussels) are the most important prey items. In the Bonavista Bay study crabs composed ~50% of the food intake and molluscs composed ~11%. In the Long Island Sound study prey items were compared on the basis of frequency of occurrence in stomachs. Crustaceans (predominantly crabs) were found in over 90% of the stomachs. Bivalve molluscs occurred in 51%. Polychaetes accounted for only 2.5% of the food intake in the Bonavista Bay study, but they were found in 59% of the Long Island Sound lobsters.

In the model the lobster food chain is represented by crabs, mussels, polychaetes, phytoplankton, and sediment detrital organic material. Polychaetes are included, even though they are a less important food source, because they provide a different route of chemical transfer to the lobster. The small crabs and mussels transfer chemical from the water column through consumption of phytoplankton. The polychaetes transfer chemical from the sediment to the lobster through their ingestion of sediment particles.

The winter flounder is an omnivore. Stomach content analyses indicate a diet that includes polychaetes, amphipod and isopod crustaceans, pelecypods, and plant material (*6*). As part of a quantitative analysis of the food habits of northwest Atlantic fish, Maurer and Bowman (*7*) found that polychaetes were the major food item, composing ~34% of stomach content weight. Coelenterates (20%) and crustaceans (7%) were the next most important food groups. Polychaetes were also found to be the most important prey item for flounder from Long Pond, Conception Bay, NF (*8*) and from mud bottoms of Long Island Sound (*9*). They were a significant prey item in a Johns Bay, ME, study (*10*), although crustaceans (principally amphipods) were a higher percentage of stomach content weight. These studies clearly indicate that benthic animals form the bulk of the diet of the winter flounder.

In the model, young-of-the-year winter flounder are assumed to consume equal percentages of phytoplankton and polychaetes. Older flounder are assumed to consume polychaetes only. The polychaetes are viewed as representatives of the variety of benthic animals that are prey

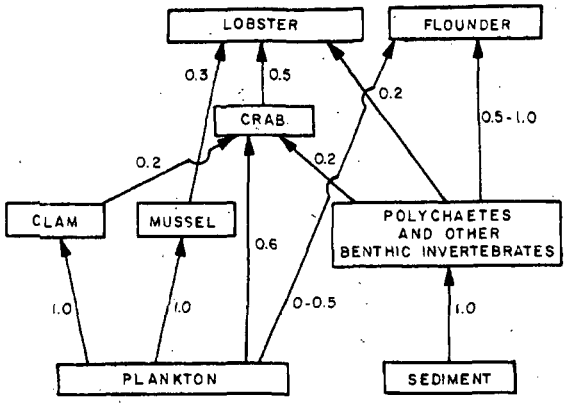

Figure 5. Food chain structure. Numbers refer to fraction of total consumption on each prey.

for the flounder. Mature flounder exhibit local onshore–offshore migration in response to temperature changes. However, migration was judged not to be significant for the less than 6-year-old animals included in the model (*3*) and was not considered.

A schematic diagram of the lobster and flounder food chains, showing the fraction of total food consumption assigned to each prey, is presented as Figure 5.

PCB Uptake Rate from Water. The rate constant K_{ui} parameterizes the transport of chemical across the gill to the blood. Its value is determined from the uptake rate for oxygen. Oxygen-transfer rate is defined by the respiration rate of the animal and the oxygen concentration of the water (c_{O_2}):

$$K_{uiO_2} = r'_i / c_{O_2} \tag{2}$$

where r'_i is the respiration rate [in units g of O_2/g(w)·day]. Mechanistically this uptake rate may be described in terms of a mass-transfer rate constant at the gill (K_{LiO_2}), the gill surface area (A), and the weight of the animal, W:

$$K_{uiO_2} = K_{LiO_2} A / W \tag{3}$$

Similarly, the mass-transfer rate for a chemical is

$$K_{ui} = K_{Li} A / W \tag{4}$$

If eqs 2 and 3 are equated, solved for A/W, and substituted into eq 4, the uptake rate of the chemical may be written as

$$K_{ui} = \frac{K_{Li}}{K_{LiO_2}} \frac{r'_i}{c_{O_2}} \tag{5}$$

From this equation it follows that the uptake rate of a chemical can be computed from the respiration rate of the animal if the ratio of the mass-transfer coefficients for the chemical and oxygen is known. Expressions relating these coefficients to characteristics of the chemical and the physiology of the animal have been developed (*11–13*). Estimates of the ratio may also be obtained from measurements of chemical and oxygen uptake efficiencies. The ratio of mass-transfer coefficients is equal to the ratio of uptake efficiencies measured when the body burden of the animal is zero.

In the model the chemical/oxygen uptake efficiency ratio was assumed to be equal to 1 for all of the homologues. Measurements of oxygen and organic chemical uptake efficiencies indicate that they are approximately equal for chemicals with log K_{ow} values between about 3 and 6 (*14*). For higher K_{ow} chemicals the chemical uptake efficiency appears to decline, although little data are available to describe this decline.

PCB Excretion Rate. The excretion rate constant K_i includes all of the processes by which the animal is able to depurate chemical. For most organic chemicals it appears that the gill is the major site of depuration (*15*) and that K_{ui} and K_i define the rates of uptake and elimination for a reversible diffusive process. The ratio of these rate constants defines the equilibrium condition for this process, or what is generally called the bioconcentration factor, N.

It has been demonstrated that the bioconcentration factor of neutral organic chemicals measured in laboratory studies can be predicted from the K_{ow} of the organic chemical (*16–19*). In fact, it appears that the lipid-normalized bioconcentration factor is approximately equal to K_{ow}, at least for log K_{ow} values up to ~6. Therefore, it is possible to compute N for a neutral organic chemical from the K_{ow} of the chemical and the fraction lipid of the animal (f_L), i.e.:

$$N_i = f_{Li} K_{ow} \tag{6}$$

With this value of N for animal i in the food chain and the computed value of K_{ui}, it is then possible to compute K_i:

$$K_i = K_{ui} / N_i \tag{7}$$

Above a log K_{ow} value of 6 a loss of linearity has been observed in correlations of N and K_{ow} (20–22). N appears to reach a maximum in the log K_{ow} range 6.5–7 and begins to decrease at higher log K_{ow} values. Several hypotheses exist to explain this behavior. Gobas et al. (*15*) have reviewed and evaluated these hypotheses and have concluded that the dominant effects are the increasing importance of fecal elimination and a decrease in freely dissolved chemical (due to complexation with dissolved and colloidal organic material) as K_{ow} increases. The latter effect is an experimental artifact dependent on the concentration of organic matter in the water used in the experiment. Fecal elimination was shown to lower the slope of the N–K_{ow} relationship but not cause a decreasing relationship.

Bioconcentration factors for PCB homologues 3–5 were computed from eq 6 by using the average measured lipid content of each species (Table I) and assumed log K_{ow} values of 5.5, 6.0, and 6.5, respectively. To reflect the observed loss of linearity of the N–K_{ow} relationship, the value for homologue 6 was assumed to be equal to that of homologue 5.

Food Consumption Rate. The rate of consumption of food C_i is calculated from the rate of energy usage. Energy usage is estimated from the rates of production and metabolism of body tissue by the animal. Growth rate defines the net production of body tissue [g(w) (g(w))$^{-1}$ day^{-1}]. The rate of metabolism of body tissue, R_i, may be computed from the respiration rate by (1) stoichiometrically converting respiration from g of O_2 (g(w))$^{-1}$ day^{-1} to g of C (g(w))$^{-1}$ day^{-1}, (2) converting carbon to dry weight by assuming all animals are 40% carbon on a dry weight basis, and (3) converting dry weight to wet weight by using observed ratios. Given the caloric density of the animal's tissue [in units of cal/g(w)], λ_i, the energy usage rate, P_i, is then

$$P_i = \lambda_i (R_i + G_i) \tag{8}$$

Dividing P_i by the fraction of ingested energy that is assimilated, a, yields the rate of energy intake by the animal.

Table I. Bioenergetic Related Parameters Used in Food Chain Model Calibration

species	age, yr	growth rate (1/day), g	respiration rate R,[a] g(w) (g(w))$^{-1}$ day	food assim. eff, a	frac. lipid, f_L	frac. dry
polychaete		0.0070	0.02	60	0.015	0.20
clam		0.0080	$0.014e^{0.085T}$	45	0.003	0.20
mussel		0.0019	$0.012e^{0.036T}$	45	0.009	0.20
crab		0.0090	0.009	45	0.008	0.25
flounder (0.01 g at birth)	0–1	0.0130	$0.0046W^{-0.24}e^{0.067T}$	80	0.018	0.25
	1–2	0.0063				
	2–3	0.0017				
	3–4	0.0009				
	4–5	0.0004				
	5–6	0.0004				
lobster (0.05 g at birth)	0–1	0.0087	$0.0035W^{-0.13}e^{0.066T}$	80	0.008	0.25
	1–2	0.0085				
	2–3	0.0039				
	3–4	0.0024				
	4–5	0.0015				
	5–6	0.0013				

[a] W, weight (g); T, temperature (°C).

The rate of consumption of food, C_{ij}, is the energy intake rate divided by the caloric density of the food, λ_j:

$$C_{ij} = \frac{\lambda_i}{\lambda_j}\frac{R_i + G_i}{a} \tag{9}$$

Where food is a lower trophic level animal, differences in caloric density were assumed to be related to differences in the wet weight/dry weight ratio; i.e., the caloric density of dry tissue was assumed to be the same for predator and prey. The caloric density ratio in eq 9 was thus replaced by the ratio of the dry weight fractions of the predator and its prey. Doing this ignores differences in body composition, particularly differences in lipid content. While such differences do effect the caloric density ratio, they are much less significant than the effect of differences in water content.

For deposit feeding animals consumption was based on carbon rather than energy. C_i was computed as above except that caloric density was not considered, P_i was expressed as g of C (g(w))$^{-1}$ day^{-1} by using the conversion factors mentioned above, and food assimilation efficiency, a, was interpreted as the fraction of ingested carbon that is assimilated. In the application of eq 1, υ_j, the chemical concentration in the food (i.e., sediment), was expressed as μg/g of C.

The assimilation efficiency of food is a function of the type of food eaten and the rate of consumption. In general, efficiencies are near 0.8 for carnivorous species and 0.3 for herbivorous species (*23*). Values reported for filter feeders such as the hard clam and the mussel are in the range of 0.3–0.6. In a summary of adsorption efficiency data Bayne and Newell (*24*) reported values for *Mytilus edulis* ranging from 0.36 to 0.6. Tenore and Dunstan (*25*) and Bricelj et al. (*26*) have reported organic material assimilation efficiencies for the hard clam in the range of 0.7–0.8, which is equivalent to ~0.3 on a dry weight basis. Deposit feeders appear to have efficiencies in the range of the herbivorous species (*27*), although values vary greatly across studies. On an organic carbon basis, measured efficiencies range from about 0.05 to 0.8, depending on the material ingested. High values have been obtained from algae (*28*) whereas low values appear to reflect more refractory carbon sources such as sea grass detritus (*29*).

In the model, assimilation efficiencies were assumed to be 0.8 for the lobster and winter flounder and 0.45 for the crab, hard clam, and the mussel. A low value is used for the crab since the crabs assumed to be prey for the flounder and lobster are the herbivorous to omnivorous juvenile animals. Polychaete assimilation efficiency of sediment organic carbon was assumed to be 0.6.

Respiration and Growth Rates. The formulations used to describe respiration and growth are the same as used in previous applications of the food chain model; a weight- and temperature-, T, dependent respiration rate of the form

$$R = \beta W^{\gamma} e^{\rho T} \tag{10}$$

and an exponential growth rate (see ref 1). The respiration–weight–temperature function for each species was determined by regression of data from laboratry respiration studies. The growth rates were established from field observed length–weight, length–age, and weight–age relationships (a discussion of the analysis of the respiration and growth data is given in ref 3). The first 6-year classes of winter flounder and lobster were modeled and growth rates were determined separately for each. All other species were represented by single compartments characterized by one weight, respiration rate, and growth rate. The values used to describe respiration and growth are presented in Table I.

Assimilation Efficiency for Ingested PCBs. Several laboratory studies have examined the fraction of ingested PCB that is absorbed. Tanabe et al. (*30*) found that small carp (28 g at start of study) fed a commerical food pellet contaminated with PCBs had adsorption efficiencies ranging from 67 to 93%. The values tend to decrease with increasing chlorine content of the PCB.

Goerke and Ernst (31) fed the sandworm *Neries virens* pieces of *Lanice conchilega* contaminated with three PCB congeners for a 3-week period. Based on the PCB in the worms at the end of the exposure period, assimilation efficiencies were computed. The values were 58% for 2,5,4′-trichlorobiphenyl, 70% for 2,2′-dichlorobiphenyl, and 93% for 2,4,6,2′,4′-pentachlorobiphenyl.

Absorption efficiencies of individual PCB congeners by 900-g rainbow trout exposed to a single oral dose administered in a gelatin capsule inserted in the stomach were reported by Niimi and Oliver (*32*). The efficiencies were calculated by comparing the administered dose to the PCB estimated to be in the fish after administration. PCB in the fish was computed by extrapolation of body burden vs time data to the day of administration. The efficiencies average ~75‰ and range from 62 to 85‰. No trend with

homologue grouping was evident.

Analyzing body burden data with a first-order model, Opperhuizen and Schrap (33) estimated the assimilation efficiencies of 2,2′,3,3′,5,5′-hexa and 2,2′,3,3′,4,4′,6,6′-octachlorobiphenyl in 70–130 mg guppies fed a contaminated diet. Several concentrations of the PCBs in Tetramin fish food were used. The mean assimilation efficiencies at food PCB concentrations up to 150 μg/g ranged from 44 to 53% for the hexa- and 45 to 50% for the octachlorobiphenyl.

In a series of studies with goldfish and guppies (*20, 34, 35*), assimilation efficiencies were measured for several PCB congeners. These data indicate a decline in assimilation efficiency at the highly chlorinated congeners. For the di- through hexachlorobiphenyls no trend is evident and the values range from 42 to 67%. The measurements for an octachlorobiphenyl range from 31 to 40%, and for decachlorobiphenyl they range from 19 to 26%.

The PCB assimilation efficiency values reported in the above studies range from about 20 to 90%. For congeners in homologue groups 3–6, the range is from about 40 to 90% with little evidence of a dependency on K_{ow}. Differences between studies may be related to the use of different sizes and species of animals and to differences in the type of food used. Because of the evident large uncertainty in this parameter and the sensitivity of the model to its value, appropriate values for each animal and each PCB homologue were not established a priori. Rather, the experimental data were used to define an appropriate parameter range as a guide in model calibration.

Partitioning of PCBs to Phytoplankton. During initial calibration the partition coefficient (or bioconcentration factor) for plankton was dependent on K_{ow}, as defined by eq 6. This caused computed penta- and hexachlorobiphenyl concentrations in the higher trophic levels to exceed observed levels, even at the lower bounds of observed assimilation efficiencies. Subsequent review of published data indicated that the plankton bioconcentration factor is approximately constant over the full range of PCB congeners. Figure 6A shows the bioconcentration factors for various PCB congeners in Lake Ontario plankton. These data were reported by Oliver and Niimi (*36*). It appears that the BCF is independent on K_{ow} in the log K_{ow} range of 5–8. Laboratory phytoplankton BCF data for PCB congeners (*39–41*) and other organic chemicals (*42*) suggest that BCF is proportional to K_{ow} up to log K_{ow} or ~5 and becomes fairly constant at higher K_{ow} values (Figure 6B). Thomann (*37*) has shown that, for a generic food chain, varying the plankton partition coefficient–K_{ow} relationship between independence and linear dependence dramatically alters the bioaccumulation factors of high K_{ow} chemicals.

Recent laboratory experimental studies (Debra Swackhammer, University of Minnesota, unpublished data) suggest that the depression of phytoplankton BCF below its expected relationship to K_{ow} is related to growth rate. These data show that as growth rate is decreased the BCF values approach the values defined by eq 6. The mechanisms controlling the BCF–growth relationship have not been elucidated. It is possible that the release of organic carbon by phytoplankton (i.e., exudation) provides a mechanism of chemical loss that depresses the BCF. Exudation has been shown to be related to the rate of primary production and thus to the growth rate.

Alternately, it is possible that the observed BCF–K_{ow} relationship is an artifact caused by the use of total dissolved chemical, rather than bioavailable dissolved chemical, in the BCF calculation. Dissolved or colloidal organic matter present in the water would decrease the bioavailable fraction of measured dissolved chemical in proportion to its concentration and the K_{ow} of the chemical. Such a "third phase" is known to cause apparent independence of partitioning and K_{ow}. Total dissolved PCB measurements were used in this work and the third phase effect would be included in the BCF calculations.

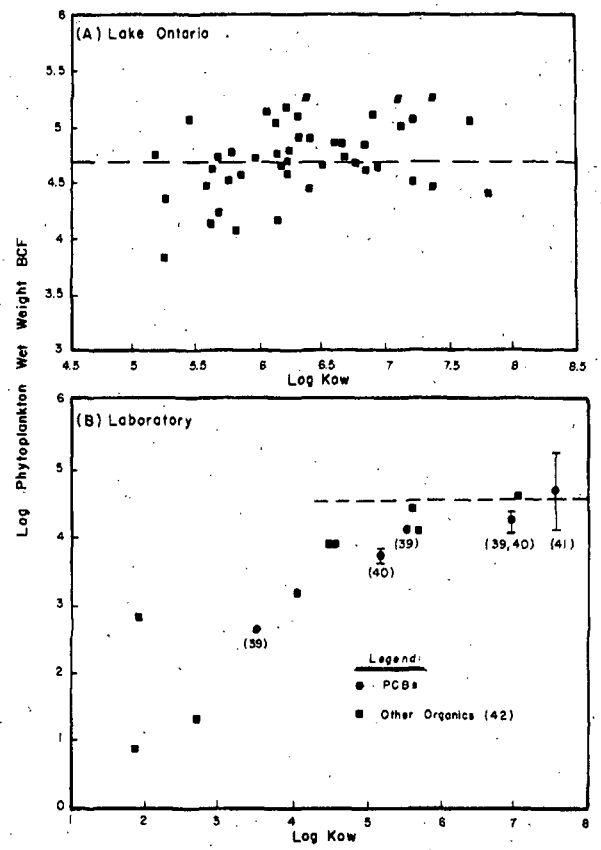

Figure 6. Relationship of phytoplankton BCF and K_{ow} for (A) PCB congener field data from Lake Ontario (*36*) and (B) laboratory data for PCBs (*39–41*) and other organic chemicals (*42*). Horizontal line shows value used in the model for tri- through hexachlorobiphenyl.

Consistent with the Lake Ontario data, a wet weight based log BCF of 4.6 was used in the calibration of the food chain model.

Model Calibration. The final calibrations are the results of model runs to determine a consistent set of parameters that are in agreement with literature or laboratory values and reproduce the observed average PCB concentrations reported during the sampling cruises in 1984 and 1985.

Arithmetic averages over all size classifications were used in comparing the observed and computed concentrations. The averages of the computed flounder and lobster concentrations were weighted so that the contribution of any age class to the average was consistent with the contribution of that age class to the average of the observed values. For all other species the steady-state computed concentration was compared to the arithmetic average observed concentration. Six age classes of flounder and lobster were included in the model based on the weights of the animals collected during the trawls. The largest flounder age class included animals weighing up to 363 g and the largest lobster age class included animals weighing up to 773 g. A few larger animals were reported in the trawl data; however, they were not included in the data

Table II. Chemical Assimilation Efficiencies Used in PCB Calibrations

species	chem assim eff, % homologue 3	4	5	6	total PCB
polychaete	60	25	15	15	15
clam	50	30	20	20	20
mussel	50	30	20	20	20
crab	50	40	25	25	25
lobster	50	40	25	25	25
flounder	80	60	40	40	40

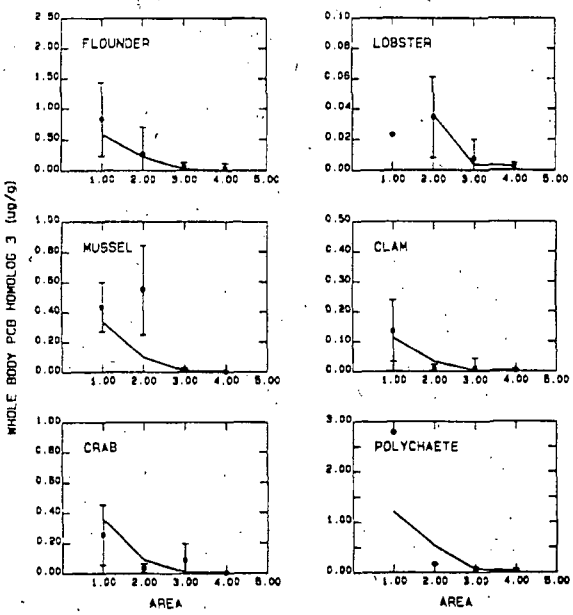

Figure 7. Observed and computed PCB homologue 3 concentrations in New Bedford Harbor animals. Computed values are indicated by the line.

averages. Lobster were not modeled in area 1 since only a single lobster was collected during the cruises.

The food chain model was calibrated for homologues 3–6 and for total PCB. Total PCB was computed two ways. First, the summation of the concentrations computed for the homologues was compared to the observed total PCB as an additional check on the homologue calibrations. Second, total PCB was calibrated as a separate chemical. The area average water column and sediment exposure concentrations were used in the calibration. The exposure concentrations determined from the cruise data were assumed to represent the average over the life span of the animals. Such an assumption is reasonable, based on the relatively constant body burdens observed between the late 1970s and the time of the cruises (*3*).

During calibration we restricted changes in assimilation efficiency to maintain a relationship of assimilation efficiency and homologue that was consistent across all of the species in the food chain. This restriction reflects the fact that the transfer of any homologue across the gut of any animal is controlled by processes that are chemical dependent, such as lipid solubility, molecular size, and molecular diffusivity. Therefore the relationship of assimilation efficiency and homologue should be similar for all of the animals. This restriction coupled with a priori specification of a constant gill oxygen/PCB mass-transfer coefficient ratio across homologues at a value of 1 (the model is rather insensitive to this assumption because

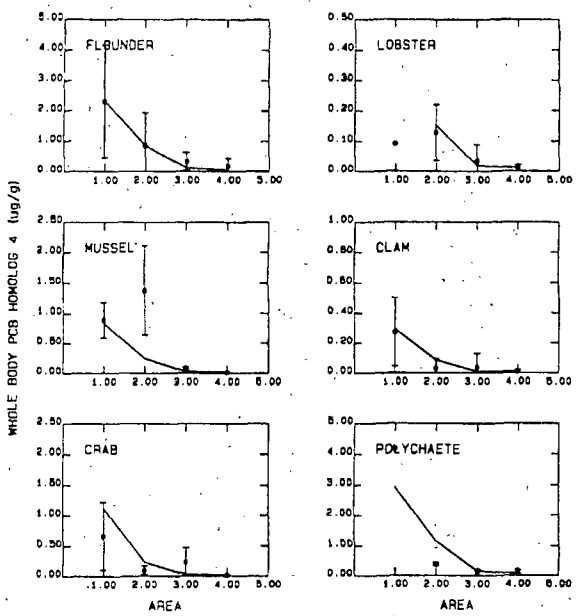

Figure 8. Observed and computed PCB homologue 4 concentrations in New Bedford Harbor animals. Computed values are indicated by the line.

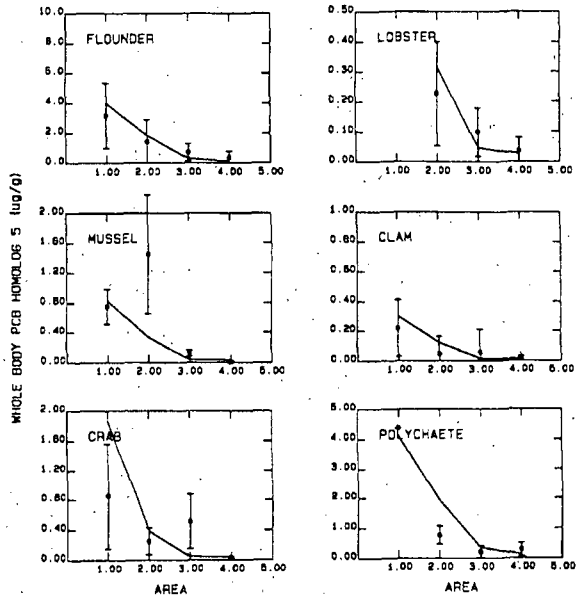

Figure 9. Observed and computed PCB homologue 5 concentrations in New Bedford Harbor animals. Computed values are indicated by the line.

uptake from food dominates accumulation of the higher chlorinated homologues) and a priori calculation of BCF from animal lipid content and K_{ow} allows for little parameter adjustment during the calibration process. The extent to which the model reproduces the observed concentrations is thus viewed as a rigorous test of the modeling framework. The calibration values of assimilation efficiency are presented in Table II.

The comparisons between observed and calculated concentrations are presented in Figures 7–11 for homologues 3–6 and total PCB as the sum of these homologues and in Figure 12 for the separate total PCB calibration. Both the observed and calculated values are averaged over

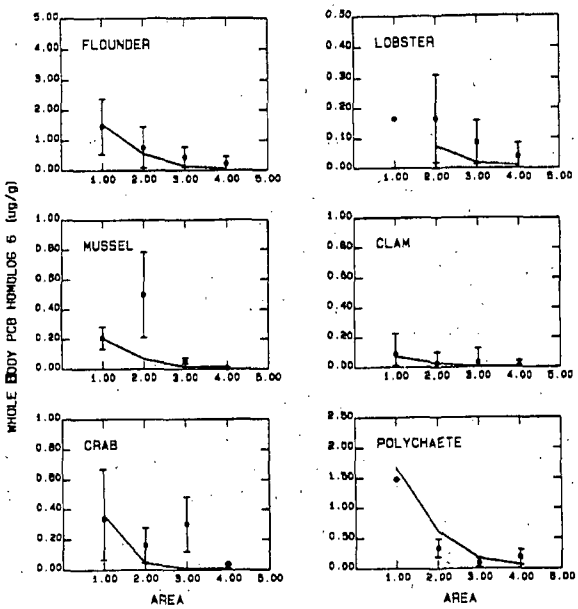

Figure 10. Observed and computed PCB homologue 6 concentrations in New Bedford Harbor animals. Computed values are indicated by the line.

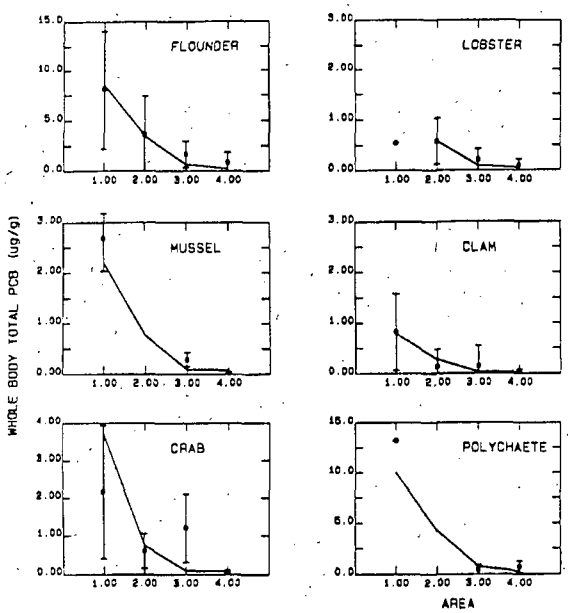

Figure 11. Observed and computed total PCB (as sum of homologues 3–6) concentrations in New Bedford Harbor animals. Computed values are indicated by the line.

all age classes. The observed values are arithmetic means and standard deviations of the combined cruise data.

There is generally good agreement between the observed data and the calculated concentrations for the homologues and total PCB. The model successfully reproduces the variation in body burdens across the homologues and over the entire food chain. It also reproduces the spatial concentration gradients evident in the data, although some bias is evident in areas 3 and 4. In these areas the computed values fall within the range of the data but they are consistently below the mean. It was not possible to achieve a calibration that eliminated this bias without computing unreasonably high concentrations in areas 1 and 2. The

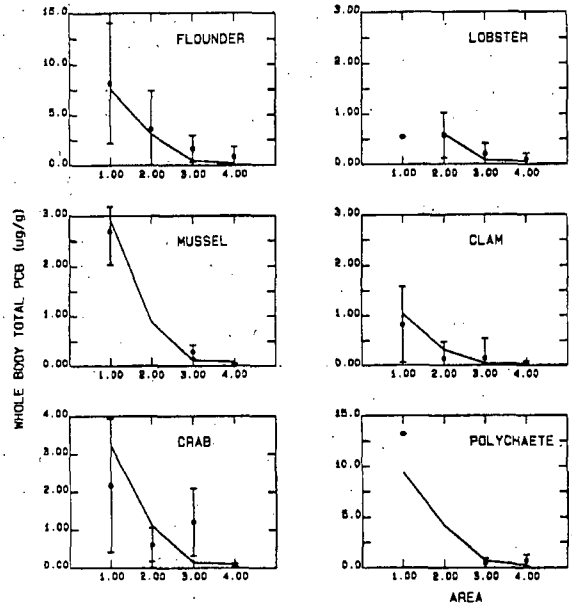

Figure 12. Observed and computed total PCB (as a separate calibration) concentrations in New Bedford Harbor animals. Computed values are indicated by the line.

data from areas 3 and 4 may reflect a sampling bias to nearshore or shallow areas that are more highly contaminated than the stations from which water and sediment samples were taken. Because of the greater significance of model calculations in the more contaminated areas 1 and 2, the calibration was directed to these areas.

Factors Controlling PCB Concentrations in Biota

Assimilation Efficiency of Ingested PCBs. Generic models of organic chemical accumulation have indicated that above a log K_{ow} of ~5–6 food is the dominant source of chemical to the food chain (*37*, *38*). This occurs because as a chemical becomes more hydrophobic and lipophilic its concentration in the plankton and sediment that constitute the base of the food chain becomes increasingly greater than its concentration in the water.

In New Bedford Harbor the contribution from food is species dependent and is calculated to be more significant for flounder than for lobster. Fifty-five percent of lobster trichlorobiphenyl is from food, whereas 80% of the concentration of this homologue in flounder is from food. These percentages increase to about 80 to 95%, respectively, for hexachlorobiphenyl. Differences between the species are attributable to differences in the contribution from the more highly contaminated benthic component of the food chain.

Because food constitutes the major vector of contamination, assimilation efficiency of ingested chemical is a controlling parameter in the model. Successful calibration required that assimilation efficiency declines as PCB chlorination increases. Although our review of published laboratory measurements of assimilation efficiency of PCB congeners suggests a decline, the data show little trend below K_{ow}s representative of the hexachlorobiphenyl congeners. Thus, an inconsistency exists between the values used in the model and those calculated from laboratory experimental data.

The assimilation efficiency values used in modeling trichlorobiphenyl are in agreement with the experimental data. The values used for the higher chlorinated homologues fall below the range of the experimental data. It

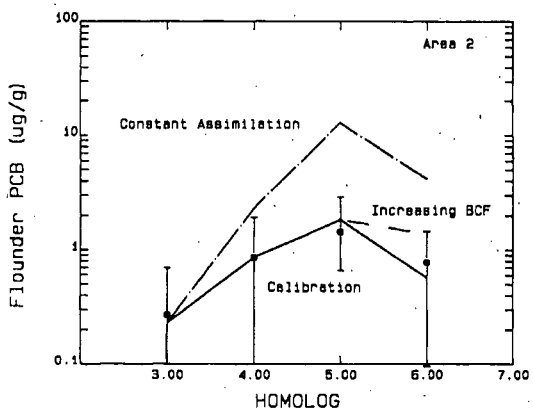

Figure 13. Comparison of observed area 2 flounder PCB with values computed by the calibration and by assuming either that the assimilation efficiency is constant or that the log BCF of hexachlorobiphenyl is 0.5 unit above that of tetrachlorobiphenyl.

was not possible to successfully calibrate the model while maintaining assimilation efficiencies constant at levels used for trichlorobiphenyl. To illustrate this point a comparison of observed and computed area 2 flounder PCB homologue concentrations is presented in Figure 13. Computed concentrations for the calibrated model and when assimilation efficiencies are held constant for all homologues are shown. Using constant assimilation efficiencies in the calibrated model results in computed flounder penta- and hexachlorobiphenyl concentrations that are about 1 order of magnitude too high. The uncertainty in the bioenergetic parameters (respiration and growth) is much too small to account for the overprediction at constant assimilation efficiency. Adjustments of the gill mass-transfer rate constants or the excretion rate constants also do not significantly reduce the computed concentrations since, at the higher K_{ow} levels, the model is relatively insensitive to these parameters (see discussion of excretion rate below).

The reduction in assimilation efficiency signifies a reduction in the bioavailability of the chemical to which the animal is exposed. Because the reduction is applied across the entire food chain it cannot be explained by a reduction in the bioavailability of the chemical concentrations at the base of the food chain, i.e., dissolved water column and sediment concentrations. Also, the model computes phytoplankton PCB concentration with a constant BCF that presumably accounts for a reduction in bioavailability due to complexation of dissolved PCBs.

Thus, the model has suggested that the decline in assimilation efficiency of PCBs that has been experimentally estimated to begin at log K_{ow}s greater than ~6.5–7 is consistent with field data but that it must begin at much lower K_{ow} values. Within the constraints of the model other hypotheses cannot explain the observed biota PCB concentrations in relation to the observed water and sediment PCB concentrations. The decline in assimilation efficiency is forced by the data and is not the result of the particular parameter set used in the calibration.

Application of the food chain model to other field sites is needed to confirm the relationship established here. If the relationship is real, the published experimental data may not have shown it because few studies have mimicked natural conditions with regard to feeding rate, prey species, and methods of prey contamination. These types of studies need to be conducted.

Excretion of PCBs. Although uptake of PCBs from water is of minor significance, especially for the higher chlorinated congeners, the gill oxygen/chemical transfer efficiency ratio can still be important to accumulation because the gill is the primary site of excretion. This parameter and the bioconcentration factor define the excretion rate. However, because excretion rate decreases as PCB chlorine level increases, growth becomes a significant component of concentration loss rate at the higher chlorinated homologues. As a result, the model is less sensitive to assumptions about excretion of the higher homologues than it is to assumptions about PCB assimilation efficiency. For example, if the assumption of a constant excretion rate for homologues 5 and 6 that was used in calibration is replaced by a declining rate consistent with the linear BCF–K_{ow} relationship, only a slight increase in body burden is calculated. For flounder this factor of 3 decline in excretion rate increases hexachlorobiphenyl concentration by a factor of ~2 whereas, the factor of 2–3 increases in hexachlorobiphenyl assimilation efficiency resulting from maintaining a homologue-independent efficiency increases concentration by a factor of 10 (Figure 13).

Benthic Component of the Food Chain. Lobster and flounder accumulate PCBs from the water column by direct uptake across the gill and by feeding on animals whose PCB burden is derived from the water column. They also accumulate PCBs from the sediment by feeding on animals whose PCB body burden is derived from the sediment. For both species the benthic component of their food chains is a significant source of contamination. About 75, 83, 91, and 94% of the tri-, tetra-, penta-, and hexachlorobiphenyl concentrations in flounder are from the sediment. Lobster are computed to obtain about 35, 42, 53, and 65% of their body burdens of these homologues from the sediment. The percentages increase as homologue increases because the contribution of food to body burden is increasing.

The sediment contributes about twice as much to the body burden of flounder than it does to lobster. This difference results from differences in the structure of the food chains of these animals. The flounder diet, with the exception of the first age class, is assumed to be exclusively polychaetes, whereas only 20% of the lobster diet is polychaetes. The fraction of lobster PCB that is obtained via the benthic food chain component (35–65%) exceeds the benthic fraction of the lobster diet. This is a consequence of PCB concentrations being higher in the sediment than in the water column. As indicated earlier, sediment total PCB concentrations in areas 1–4 are 360, 160, 25, and 10 μg/g of C. The phytoplankton PCB concentrations computed from the assumed BCF and observed dissolved water column PCB concentrations [assuming 0.1 g(d)/g(w) and 0.4 g of C/g(d)] are 70, 20, 3, and 2 μg/g of C, values slightly lower than the measured water column particulate PCB concentrations presented earlier. Thus, the base of the benthic food chain is ~5–10 times higher in concentration than the base of the water column food chain.

The greater contamination in the sediment is also partially responsible for computed and observed whole body concentrations in flounder being higher than in the lobster. The higher whole body lipid content of the flounder also contributes to this difference.

Conclusions

Although the food chain model may be regarded as a complex calculation, the majority of its complexity is associated with chemical-independent parameters that define the structure of the food chain and the bioenergetics of the species. The successful application of the model to

multiple chemicals that span a wide range of bioaccumulation characteristics indicates that these biological parameters describe the food chains reasonably well. In addition, a single set of the chemical-specific parameters was sufficient for reasonable calibration to biota concentrations across the 2 order of magnitude spatial gradients in PCB exposure concentrations of New Bedford Harbor, affirming the basic validity of the modeling framework used and its utility as a predictive tool.

The model includes three chemical specific parameters; chemical/oxygen transport efficiency ratio at the gill, bioconcentration factor, and assimilation efficiency of ingested chemical. Of these, assimilation efficiency is by far the most significant in determining the extent of accumulation of hydrophobic chemicals such as the PCBs. This efficiency apparently declines from relatively high values (0.5–0.8) for trichlorobiphenyl to relatively low values (0.15–0.4) for hexachlorobiphenyl. Because this decline is not consistent with previously published experimental data it should be confirmed by application of the model to other field data sets and by conducting laboratory assimilation efficiency studies using exposure scenarios representative of natural conditions.

Chemical/oxygen transfer efficiency ratio and bioconcentration factor are important parameters for the lower chlorinated homologues whose accumulation depends significantly on uptake of chemical from water and excretion rate. However, the dominance of food as the vector of contamination and the decrease of excretion rate to levels below growth rate reduce the importance of these parameters in the accumulation of the penta- and hexachlorobiphenyl homologues.

Contaminated food provides most of the PCB observed in lobster and flounder, accounting for from 55 to 80% in lobster and 80 to 95% in flounder. The percentages increase with homologue.

Both the water column and sediment serve as PCB sources for the biota. Flounder PCB is derived mostly from the sediment, with the percentage contribution increasing from 75% for trichlorobiphenyl to 94% for hexachlorobiphenyl as the contribution from food increases. For lobster, the sediment accounts for 35% of trichlorobiphenyl increasing to 65% of hexachlorobiphenyl. The significance of the sediment relative to the water column is enhanced because the sediment is more contaminated than the water column. This difference in contamination makes specification of feeding habits an important aspect of the model. Thus, the validity of the conclusions is somewhat dependent on the accuracy of the split between the prey species. This split is not as critical for purely pelagic or purely benthic food chains.

Whole body PCB concentrations in flounder exceed those in lobster. The model indicates that these differences occur because of the flounder's higher whole body lipid content and because its food chain is more closely associated with the more highly contaminated sediment.

Acknowledgments

Maureen Casey and Leslie Sparrow of HydroQual participated in the data analysis and model calibration. John St. John of HydroQual directed the project from which this work is derived. The support of the Battelle Project Manager Richard McGrath is also gratefully acknowledged. This paper benefited greatly from reviews by my colleagues Dominic DiToro and Robert Thomann and by two anonymous reviewers.

Registry No. Trichlorobiphenyl, 25323-68-6; tetrachlorobiphenyl, 26914-33-0; pentachlorobiphenyl, 25429-29-2; hexachlorobiphenyl, 26601-64-9.

Literature Cited

(1) Thomann, R. V.; Connolly, J. P. *Environ. Sci. Technol.* 1984, *18*, 65.
(2) Connolly, J. P.; Tonelli, R. *Estuarine, Coastal Shelf Sci.* 1985, *20*, 349.
(3) Battelle Ocean Sciences. *New Bedford Harbor Modeling Program Final Report*; United States Environmental Protection Agency: Boston, MA, 1990.
(4) Ennis, G. P. *J. Fish. Res. Board Can.* 1973, *30*, 1905.
(5) Weiss, H. M. Ph.D. Thesis, The University of Connecticut, 1970.
(6) Klein-MacPhee, G. Synopsis of biological data for the winter flounder, *Pseudopleuronectus americanus* (Walbaum). NOAA Technical Report NMFS Circular 414, 1978.
(7) Maurer, R. O., Jr.; Bowman, R. E. Food habits of marine fishes of the northwest Atlantic—Data Report. Woods Hole R.D. No. 75-3, 1975.
(8) Kennedy, V. S.; Steele, D. H. *J. Fish. Res. Board Can.* 1971, *28*, 1153.
(9) Richards, S. W. *Bull. Bingham Oceanogr. Collect. Yale Univ.* 1963, *18*.
(10) Hacunda, J. S. *Fish. Bull.* 1981, *79*, 775.
(11) Gobas, F. A. P. C.; Opperhuizen, A.; Hutzinger, O. *Environ. Toxicol. Chem.* 1986, *5*, 637.
(12) Gobas, F. A. P. C.; Mackay, D. *Environ. Toxicol. Chem.* 1987, *6*, 495.
(13) Barber, M. C.; Suarez, L. A.; Lassiter, R. R. *Environ. Toxicol. Chem.* 1988, *7*, 545.
(14) McKim, J. M.; Schnieder, P.; Vieth, G. *Toxicol. Appl. Pharmacol.* 1985, *77*, 1.
(15) Gobas, F. A. P. C.; Clark, K. E.; Shiu, W. Y.; Mackay, D. *Environ. Toxicol. Chem.* 1989, *8*, 231.
(16) Tulp, M.; Hutzinger, O. *Chemosphere* 1978, *10*, 849.
(17) Neely, W. B. *Environ. Sci. Technol.* 1979, *13*, 1506.
(18) Veith, G. D.; DeFoe, D. L.; Bergstedt, B. V. *J. Fish. Res. Board Can.* 1979, *36*, 1040.
(19) Mackay, D. *Environ. Sci. Technol.* 1982, *16*, 274.
(20) Bruggeman, W. A.; Opperhuizen, A.; Wijbenga, A.; Hutzinger, O. *Toxicol. Environ. Chem.* 1984, *7*, 173.
(21) Opperhuizen, A.; Van De Velde, E. W.; Gobas, F. A. P. C.; Liem, D. A. K.; Van der Steen, J. M. D.; Hutzinger, O. *Chemosphere* 1985, *14*, 1871.
(22) Gobas, F. A. P. C.; Shiu, W. Y.; Mackay, D. In *QSAR in Environmental Toxicology II*; Kaiser, K. L. E., Ed., D. Reidel Publishing Co.: Dordrecht, The Netherlands, 1987; p 107.
(23) Brett, J. R.; Groves, T. D. D. In *Fish Physiology*; Hoar, W. S., Randall, D. J., Brett, L. R., Eds., Academic Press: New York, 1979; Vol. 8, p 280.
(24) Bayne, B. L.; Newell, C. M. *Mar. Ecol. Prog. Ser.* 1980, *3*, 317.
(25) Tenore, K. R.; Dunstan, W. M. *Mar. Biol.* 1973, *21*, 190.
(26) Bricelj, V. M.; Bass, A. E.; Lopez, G. R. *Mar. Ecol. Prog. Ser.* 1984, *17*, 57.
(27) Yingst, J. Y. *J. Exp. Mar. Biol. Ecol.* 1976, *23*, 55.
(28) Forbes, V. E.; Lopez, G. R. *J. Exp. Mar. Biol. Ecol.* 1989, *126*, 181.
(29) Levinton, J. S.; Stewart, S. *Mar. Ecol. Prog. Ser.* 1988, *49*, 259.
(30) Tanabe, S.; Maruyama, K.; Tatsukawa, R. *Agric. Biol. Chem.* 1982, *46*, 891.
(31) Goerke, H.; Ernst, W. *Chemosphere* 1977, *9*, 551.
(32) Niimi, A. J.; Oliver, B. G. *Can. J. Fish. Aquat. Sci.* 1983, *40*, 1388.
(33) Opperhuizen, A.; Schrap, S. M. *Chemosphere* 1988, *17*, 253.
(34) Bruggeman, W. A. Ph.D. Thesis, University of Amsterdam, 1980.
(35) Bruggeman, W. A.; Martron, L. B. J. M.; Kooiman, D.; Hutzinger, O. *Chemosphere* 1981, *10*, 811.
(36) Oliver, B. G.; Niimi, A. J. *Environ. Sci. Technol.* 1988, *22*, 388.
(37) Thomann, R. V. *Environ. Sci. Technol.* 1989, *23*, 699.

(38) Connolly, J. P.; Pedersen, C. J. *Environ. Sci. Technol.* **1987**, *22*, 99.
(39) Geyer, H.; Viswanathan, R.; Freitag, D.; Korte, F. *Chemosphere* 1981, *10*, 1307.
(40) Wang, K.; Rott, B.; Korte, F. *Chemosphere* 1982, *11*, 525.
(41) Lederman, T. C.; Rhee, G. Y. *Can. J. Fish. Aquat. Sci.* **1982**, *39*, 380.
(42) Mailhot, H. *Environ. Sci. Technol.* **1987**, *21*, 1009.

Received for review July 20, 1990. Revised manuscript received November 9, 1990. Accepted December 10, 1990. This work was carried out at HydroQual, Inc. under subcontract to Battelle Ocean Sciences as part of the U.S. EPA New Bedford Harbor RI/FS Modeling Program.

Evaluation of Vapor-Phase Nicotine and Respirable Suspended Particle Mass as Markers for Environmental Tobacco Smoke

Brian P. Leaderer*

John B. Pierce Laboratory, Department of Epidemiology and Public Health, Yale University School of Medicine, New Haven, Connecticut 06519

S. Katharine Hammond

Department of Family and Community Medicine, University of Massachusetts Medical School, Worcester, Massachusetts 01655

■ Vapor-phase nicotine and respirable suspended particle mass (RSP) emissions from tobacco combustion were evaluated as markers for environmental tobacco smoke (ETS) in an environmental chamber and a field study. The chamber results indicated that emissions of vapor-phase nicotine and RSP were similar among brands of cigarettes and both contaminants were emitted in quantities that are easily measured in enclosed environments. The field study collected 1-week measurements of vapor-phase nicotine and RSP as well as extensive source use information in 96 residences. Vapor-phase nicotine measurements were closely related to the number of cigarettes smoked and were highly predictive of respirable suspended particle mass generated by tobacco combustion. The observed field association between vapor-phase nicotine and RSP was consistent with chamber studies. The chamber and field studies reported here indicate that vapor-phase nicotine is a suitable qualitative and quantitative marker for environmental tobacco smoke in the residential indoor environment. Due to background levels of RSP from other sources, RSP measurements indoors should be supplemented by a measure of the quantity of tobacco consumed or a measure of the vapor-phase nicotine concentration before the portion attributable to ETS can be determined.

Introduction

The health hazards associated with smoking have received extensive study and are well-known. Thus, it is not surprising that there is now a growing concern that exposure to environmental tobacco smoke (ETS) may be associated with adverse health and comfort effects in nonsmokers. The health and comfort effects associated with involuntary smoking have been extensively reviewed in two recent reports (*1*, *2*). While both reports found an association between exposure to ETS and a wide range of acute and chronic health effects, they noted that epidemiologic studies of ETS have been handicapped due to limitations in assessing exposures to ETS. Accurate methods of assessing ETS exposures are needed for conducting epidemiologic studies, for calculating risks, and in developing effective control measures to reduce or eliminate risks.

ETS is a complex mix of over 4000 chemicals found in both the particle and vapor phase; it is primarily composed of exhaled mainstream smoke and contaminants emitted from the burning end of a cigarette between puffs. ETS is a major source of both particle- and vapor-phase indoor air contaminants (*1–3*). Some of the ETS contaminants are associated solely with the combustion of tobacco (e.g., nicotine and tobacco-specific nitrosamines) while others are emitted by a number of other sources in the outdoor and indoor environment (e.g., carbon monoxide and suspended particle mass). Given this complex mix, one necessary task is the identification of an air contaminant or class of air contaminants for monitoring that would be indicative of the presence and amount of ETS.

Over the past several years a number of marker or proxy compounds have been used to represent ETS concentrations in both field and chamber studies. Nicotine, carbon monoxide, 3-ethenylpyridine, nitrogen dioxide, pyridine, aldehydes, nitrous acid, acrolein, benzene, toluene, myosmine, and several other compounds have been used or been suggested for use as markers or proxies for the vapor-phase constituents of ETS (*1–7*). Tobacco-specific nitrosamines, particle-phase nicotine and cotinine, solanesol, polonium-210, benzo[*a*]pyrene, potassium, chromium, and respirable suspended particle (RSP) mass are among the air contaminants used or suggested for use as markers for particle-phase constituents of ETS (*1–3*, *8–10*).

Vapor-phase nicotine is a strong candidate as a marker for ETS. It is specific to tobacco combustion and emitted in large quantities in ETS. Approximately 95% of the nicotine in ETS is in the vapor phase (*1*, *2*, *4*, *5*, *11*). In addition, measurements of nicotine and one of its metabolites, cotinine, (in blood, urine, and saliva) are used extensively as a biomarkers of exposure to ETS and active smoking (*1*, *2*). Recent advances in air sampling have resulted in the development of a variety of inexpensive and accurate active (*4*, *5*, *12*, *13*) and passive (*14*) monitors for measuring nicotine in indoor environments and for personal monitoring.

ETS is a particularly important indoor source of respirable suspended particle mass (RSP particle diameter $\leq 2.5\ \mu m$). ETS particles contain a number of known and suspected carcinogens, which have also been used as proxies for ETS in both chamber and field studies (*1*, *2*). Studies of personal exposures to RSP and of RSP levels in indoor environments have shown elevated levels of RSP when ETS exposure was reported (*1*, *2*). Efforts to model ETS exposures for the purpose of assessing risks and the

 0013-936X/91/0925-0770$02.50/0 © 1991 American Chemical Society